

Low-energy spectral density for the Alexander-Anderson model

C. A. Paula, M. F. Silva, and L. N. Oliveira

Instituto de Física de São Carlos, C.P. 369, 13560-970 São Carlos, SP, Brazil

(Received 7 July 1998)

Langreth's expression relating the low-energy impurity spectral density of the Anderson model to the Fermi-level phase shift of the conduction electrons is extended to the two-impurity model. As an application, the accuracy of two numerical renormalization-group spectral-density computations are checked against the exact expression. [S0163-1829(99)01301-6]

Three decades ago, a concise argument planted a landmark in the theory of dilute magnetic alloys.¹ In his proof that the conduction-electron phase shifts for the single-impurity Anderson model obey the Friedel sum rule, Langreth obtained an expression implicitly relating the low-energy impurity spectral density to the Fermi-level phase shift. Many years later, that relation would prop the final effort that brought to light the underlying physics of the model² and check the accuracy of spectral density computations.^{3,4} To this date, it remains one of the few exact expressions describing the excitation properties of strongly correlated electrons.

In view of the extensive literature on the Alexander-Anderson model,⁵ which includes spectral density computations,⁶ it is surprising that this important expression has not been generalized. In this report we show that the combination of a few well-established results extends Langreth's analysis¹ to the two-impurity model. After deriving the expression that connects the spectral densities to the conduction-band phase shifts, we analyze numerical results in the light of the exact expression. Since the model has two widely studied versions with different properties,^{6,7} we consider data for both the symmetric and the asymmetric models. For the former version, we discuss the ground-breaking numerical renormalization-group (NRG) results in Ref. 6 and show that today's more powerful computational resources and more efficient numerical procedures yield significantly more accurate results; for the latter, we present and discuss new NRG results for the low-energy spectral density calculated at three impurity separations chosen to probe the three characteristic regimes defined by the competition between the Ruderman-Kittel-Kasuya-Yosida (RKKY) interaction and the Kondo temperature.

The Alexander-Anderson model comprises two orbitals representing two impurities, positioned at $\mathbf{R}_1 = \mathbf{R}/2$ and $\mathbf{R}_2 = -\mathbf{R}/2$, coupled to noninteracting conduction electrons representing the metallic host. Its Hamiltonian is

$$H = H_i + \sum_{\mathbf{k}\mu} \epsilon_{\mathbf{k}} c_{\mathbf{k}\mu}^\dagger c_{\mathbf{k}\mu} + V \sum_{j\mathbf{k}\mu} (d_{j\mu}^\dagger c_{\mathbf{k}\mu} e^{i\mathbf{k}\cdot\mathbf{R}_j} + \text{H.c.}), \quad (1)$$

where μ is a spin component, the Fermi operator $c_{\mathbf{k}}$ annihilates a conduction electron with momentum \mathbf{k} , and energy $\epsilon_{\mathbf{k}}$, the operator d_j ($j=1,2$) annihilates an electron at the impurity orbital at position \mathbf{R}_j , and V is the coupling between the conduction states and each impurity. The impurity

Hamiltonian, which combines the orbital energy ϵ_d with the Coulomb repulsion U between opposite-spin electrons occupying the same impurity, is

$$H_i = \sum_{j\mu} \epsilon_d d_{j\mu}^\dagger d_{j\mu} + U \sum_j d_{j\uparrow}^\dagger d_{j\downarrow}^\dagger d_{j\downarrow} d_{j\uparrow}. \quad (2)$$

To apply renormalization-group theory, we need a basis in which the impurities couple exclusively to two basis states.⁸ Unfortunately, the two states $\sum_{\mathbf{k}\mu} c_{\mathbf{k}\mu} \exp(\pm i\mathbf{k}\cdot\mathbf{R}/2)$, to which the two impurities couple in Eq. (1), respectively, are nonorthogonal. We therefore take advantage of the inversion ($\mathbf{R} \rightarrow -\mathbf{R}$) symmetry of the Hamiltonian to define an alternative basis, consisting of states that are either even (e) or odd (o) with respect to inversion:⁸

$$c_{\mathbf{k}\mu e,o} = \frac{c_{\mathbf{k}\mu} \pm c_{-\mathbf{k}\mu}}{\sqrt{2}} \quad (k_z > 0). \quad (3)$$

The restriction $k_z > 0$ avoids double counting. We likewise define symmetric combinations of impurity orbitals:

$$d_{\mu e,o} = \frac{d_{1\mu} \pm d_{2\mu}}{\sqrt{2}}. \quad (4)$$

The model Hamiltonian then becomes

$$H = \sum_{\mathbf{k}\mu p} [\epsilon_{\mathbf{k}} c_{\mathbf{k}\mu p}^\dagger c_{\mathbf{k}\mu p} + (V_{\mathbf{k}p} d_{\mu p}^\dagger c_{\mathbf{k}\mu p} + \text{H.c.})] + H_i, \quad (5)$$

where

$$V_{\mathbf{k}e} = 2V \cos(\mathbf{k}\cdot\mathbf{R}/2), \quad (6)$$

and

$$V_{\mathbf{k}o} = 2iV \sin(\mathbf{k}\cdot\mathbf{R}/2). \quad (7)$$

The following analysis depends only on the coupling between the impurities and the conduction band. The form of the impurity Hamiltonian H_i in the new basis is thus unimportant and need not be recorded.

To compute the conduction-band phase shifts δ associated with the Hamiltonian (5), we give attention to the S matrix, whose energy-shell eigenvalues are $\exp(-2i\delta)$, and to the T matrix, defined by

$$S_{\mathbf{k}p\mu,\mathbf{k}'p'\mu'} = \delta_{\mathbf{k}p\mu,\mathbf{k}'p'\mu'} - 2\pi i \delta(\epsilon_k - \epsilon_{k'}) T_{\mathbf{k}p\mu,\mathbf{k}'p'\mu'}. \quad (8)$$

As pointed out by Langreth,¹ since the conduction electrons can only scatter off the impurities, the T matrix is proportional to the impurity Green's function:

$$T_{\mathbf{k}p\mu,\mathbf{k}'p'\mu'} = V_{\mathbf{k}p}^* G_{p\mu,p'\mu'}(\epsilon_k) V_{\mathbf{k}'p'} \quad (\epsilon_k = \epsilon_{k'}), \quad (9)$$

where the Green's function is defined, as usual, by

$$iG_{p\mu,p'\mu'}(t) = \mathcal{T} \langle d_{p\mu}(t) d_{p'\mu'}^\dagger(0) \rangle. \quad (10)$$

Here \mathcal{T} is the time-ordering operator and the brackets on the right-hand side denote the ground-state expectation value.

At low excitation energies ϵ , the T matrix becomes diagonal in its parity and spin indices. To prove this, we refer to the literature on the two-impurity problem^{6,7,9,10,8} showing that, as $\epsilon \rightarrow 0$, the impurity degrees of freedom are frozen. Given that parity, charge, and spin are conserved, renormalization-group theory then shows that as $\epsilon \rightarrow 0$, the model Hamiltonian approaches the fixed point⁸

$$H^* = \sum_{\mathbf{k}\mu p} \epsilon_k c_{\mathbf{k}\mu p}^\dagger c_{\mathbf{k}\mu p} + \sum_{\mathbf{k}\mathbf{k}'\mu p} K_p c_{\mathbf{k}\mu p}^\dagger c_{\mathbf{k}'\mu p}. \quad (11)$$

Here and henceforth the primes remind us that the restriction on the right-hand side of Eq. (3) limits the momentum sums to the half-space $k_z > 0$. The constants K_p ($p = e, o$) are localized scattering potentials that determine the even- and odd-channel Fermi-level phase shifts δ_F^p . For sufficiently small couplings V , the even and the odd impurity occupations being identical, the Friedel sum rule makes the Fermi-level phase shifts symmetrical, $\delta_e^F = -\delta_o^F$; it follows that, as $V \rightarrow 0$, the effective potentials K_p must become symmetrical, $K_{e \rightarrow} = -K_{o \rightarrow}$. Additional information about these two model-parameter dependent constants can only be extracted from a full-scale diagonalization of the Hamiltonian (1).

At nonzero energies ϵ , the effective Hamiltonian (11) describes only approximately the spectrum of the model Hamiltonian (5). The deviation $H - H^*$ is nonetheless a combination of irrelevant operators. Since the most important of these make contributions of $\mathcal{O}(\epsilon)$ to the physical properties of the model, for sufficiently small energies it is safe to ignore them. The effective Hamiltonian ruling out spin-flip and parity-reversion scattering, the expression for the T matrix in Eq. (9) can be simplified:

$$T_{\mathbf{k}p\mu,\mathbf{k}'p'\mu'} = V_{\mathbf{k}'p'}^* G_{p\mu}(\epsilon_k) V_{\mathbf{k}p} \delta_{pp'} \delta_{\mu\mu'}, \quad (12)$$

where $G_{p\mu}(\epsilon)$ denotes $G_{p\mu,p\mu}(\epsilon)$. Rotational symmetry making the T matrix and the Green's function independent of μ , spin indices will henceforth be dropped.

The expression for the S matrix can likewise be simplified. With the right-hand side of Eq. (12) substituted for the T matrix, Eq. (8) becomes

$$S_{\mathbf{k},\mathbf{k}'}^p = \delta_{\mathbf{k},\mathbf{k}'} - 2\pi i \delta(\epsilon_k - \epsilon_{k'}) V_{\mathbf{k}p}^* V_{\mathbf{k}'p} G_p(\epsilon_k), \quad (13)$$

where $S_{\mathbf{k},\mathbf{k}'}^p$ is a shorthand for $S_{\mathbf{k}p\mu,\mathbf{k}'p\mu}$.

It is now straightforward to verify that the coupling coefficients $V_{\mathbf{k}p}^*$ diagonalize the S matrix.¹ The matrix multiplication of both sides of Eq. (13) by $V_{\mathbf{k}'p}^*$ yields

$$\begin{aligned} & \sum_{\mathbf{k}'} S_{\mathbf{k},\mathbf{k}'}^p V_{\mathbf{k}'p}^* \\ &= \left[1 - 2\pi i G_p(\epsilon_k) \sum_{\mathbf{k}'} \delta(\epsilon_k - \epsilon_{k'}) |V_{\mathbf{k}'p}|^2 \right] V_{\mathbf{k}p}^*. \end{aligned} \quad (14)$$

The term within square brackets on the right-hand side is the eigenvalue of $S_{\mathbf{k},\mathbf{k}'}^p$ associated with $V_{\mathbf{k}p}^*$. At the Fermi level, it follows that

$$\exp(-i2\delta_F^p) = 1 - 2\pi i G_p(\epsilon_F) \sum_{\mathbf{k}'} \delta(\epsilon_F - \epsilon_{k'}) |V_{\mathbf{k}'p}|^2. \quad (15)$$

This equation relates the impurity Green's function to the conduction phase shifts. To determine the parity-resolved spectral densities, defined by $\rho_p(\epsilon) = -(1/\pi) \sum_{\mu} \text{Im}[G_p(\epsilon)]$ ($p = e, o$), we take the real part of each side of Eq. (15) and sum over spin components. The result is

$$\rho_p(\epsilon_F) = \frac{2}{\pi \Gamma_p} \sin^2(\delta_F^p), \quad (16)$$

where

$$\Gamma_p = \pi \sum_{\mathbf{k}'} \delta(\epsilon_F - \epsilon_{k'}) |V_{\mathbf{k}'p}|^2. \quad (17)$$

Finally, we substitute the right-hand sides of Eqs. (6) and (7) for $V_{\mathbf{k}'e}$ and $V_{\mathbf{k}'o}$, carry out the sum on the right-hand side of Eq. (17), and find that

$$\Gamma_e = \pi g(\epsilon_F) V^2 \left[1 + \frac{\sin(k_F R)}{k_F R} \right], \quad (18)$$

and

$$\Gamma_o = \pi g(\epsilon_F) V^2 \left[1 - \frac{\sin(k_F R)}{k_F R} \right], \quad (19)$$

respectively, where $g(\epsilon_F)$ is the conduction density of states at the Fermi level. This completes our derivation.

Equation (16) provides a convenient test on the accuracy of numerical computations. To underscore the importance of such a check, we call the reader's attention to a recent argument,¹¹ supported by an innovative scaling procedure, questioning the generalized NRG approach employed in Ref. 8 to compute thermodynamical properties for the two-impurity Kondo model. While the numerical results showed that the low-energy thermodynamics is controlled by the ratio between the RKKY interaction and the Kondo temperature, that perturbative scaling analysis of the Kondo limit of the Anderson-Alexander model found a single characteristic energy—the Kondo temperature. From this, Fischer¹¹ inferred that the generalized NRG method yield less reliable results than those computed by the standard NRG procedure.⁶ The following comparison of the low-energy spectral densities calculated by the generalized NRG method with those predicted by Eq. (16) argues against that conclusion.

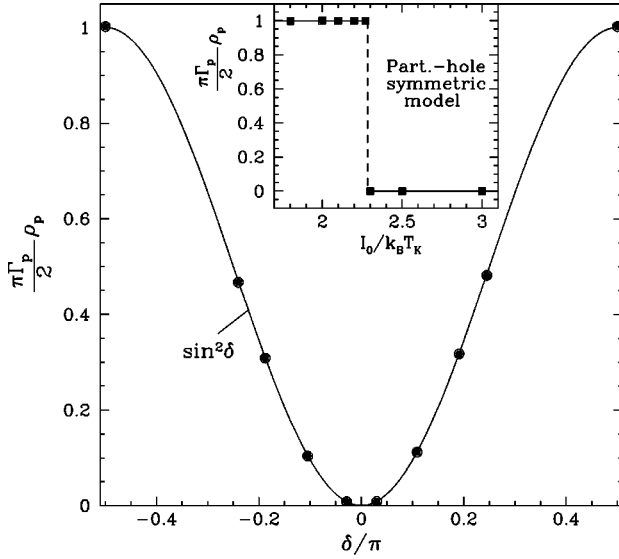


FIG. 1. Numerically computed even ($\delta < 0$) and odd ($\delta > 0$) Fermi-level spectral densities (open circles) for the asymmetrical-model parameters listed in Table I as functions of the Fermi-level phase shift δ , compared with Eq. (16). The vertical axis is normalized by the maximum density $\rho_p^{\max} = 2/\pi\Gamma_p$ ($p=e,o$), where Γ_e and Γ_o are given by Eqs. (18) and (19), respectively. For the particle-hole symmetric model, the densities (open squares) appear in the inset, as functions of the ratio between the RKKY interaction I_0 and the Kondo thermal energy $k_B T_K$. To avoid overcrowding, only the odd densities are shown. The phase shifts dropping discontinuously from $\pi/2$ to 0 as that ratio grows past a critical value $I_0/k_B T_K \approx 2.3$, Eq. (16) shows that the solid lines are the exact densities.

To this end, it is appropriate to choose model parameters representative of the limit $U = -2\epsilon_d \gg g(\epsilon_F)V^2$, in which the Alexander-Anderson model maps onto the two-impurity Kondo model with coupling constant¹²

$$J = 8V^2/U. \quad (20)$$

The conduction electrons mediate an effective (RKKY) interaction $JS_1 \cdot S_2$ between the impurity spins (S_1 and S_2) that is proportional to J^2 and, depending on the separation R , can be antiferromagnetic ($I > 0$) or ferromagnetic ($I < 0$).⁸

To calculate the even and the odd Fermi-level spectral densities for the Alexander-Anderson model, we followed the procedure in Ref. 8, with the same discretization parameter $\Lambda = 10$. This relatively large value makes a good compromise between computational effort and accuracy, the deviations¹³ in the computed densities being inferior to 1% of the maximum density allowed by Eq. (16).

Figure 1 shows the even and odd Fermi-level spectral densities for the particle-hole-asymmetric model parameters in Table I as a function of the Fermi-level phase shifts. The latter are extracted from the low-energy eigenvalues of the model Hamiltonian H : as the excitation energies approach zero, H approaches the simple fixed point described by Eq. (11), whose low-energy single-particle levels determine the Fermi-level phase shifts.^{14,8} The agreement between the numerical data (open circles) and Eq. (16) (solid line) is excellent.

TABLE I. Phase shifts δ and static spectral densities ρ for the indicated impurity separations R and effective Kondo couplings J [see Eq. (20)]. The impurity separations $R = \pi/2k_F$, π/k_F , and ∞ correspond to ferromagnetic, antiferromagnetic, and zero RKKY couplings, respectively. In all cases, the Coulomb repulsion is $U = 100D$ and the Fermi momentum $k_F = 1$. The (5% or less) discrepancy between the absolute values of the even and the odd phase shifts computed for the same model parameters are due to irrelevant operators, expected to vanish as $J \rightarrow 0$.

$k_F R$	J/D	δ_e/π	$(\pi\Gamma_e/2)\rho_e$	δ_o/π	$(\pi\Gamma_o/2)\rho_o$
$\pi/2$	0.10	-0.496	1.004	0.497	1.003
π	0.10	-0.029	0.008	0.030	0.009
π	0.14	-0.105	0.104	0.109	0.112
π	0.17	-0.188	0.309	0.191	0.317
π	0.20	-0.240	0.467	0.245	0.482
∞	0.10	-0.500	1.002	0.500	1.002

Next, we turn to a comparison with the work of Sakai and co-workers,⁶ a standard NRG procedure applied to the symmetric model obtained by substituting the momentum-independent couplings $\sum_{\mathbf{k}} V_{\mathbf{k}p} \delta(k_F - |\mathbf{k}|)$ for $V_{\mathbf{k}p}$ on the right-hand side of Eq. (5). This substitution affects the RKKY interaction, whose coefficient becomes negative-definite:⁹

$$I = -(J/D)^2 \left[\frac{\sin(k_F R)}{k_F R} \right]^2 \ln 2. \quad (21)$$

To simulate an antiferromagnetic interaction a coupling⁷

$$H_{\text{coupl}} = I_0 \mathbf{S}_1 \cdot \mathbf{S}_2 \quad (22)$$

must then be added to the model Hamiltonian. Here $I_0 > 0$ is an artificial RKKY interaction.

Particle-hole symmetry allows only two phase shifts:⁷ $\delta = 0$ or $\delta = \pi/2 \equiv -\pi/2$. There is extensive documentation for the Kondo regime showing that the phase shifts δ are $\pi/2$ for all ferromagnetic RKKY couplings $I_0 < 0$ and for sufficiently weak antiferromagnetic couplings, such that the ratio $I_0/k_B T_K$ (where T_K is the Kondo temperature) is smaller than a critical value approximately equal to 2.3.^{6,7,9} With $\delta = \pi/2$, the Fermi-level spectral densities should attain the maximum value allowed by Eq. (16),

$$\rho_p(\epsilon_F) = \frac{2}{\pi\Gamma_p}. \quad (23)$$

For larger antiferromagnetic couplings, $I_0/k_B T_K > 2.3$, the phase shifts and hence the Fermi-level spectral densities should vanish.

The numerical results in Ref. 6 agree qualitatively with these conclusions. The calculated Fermi-level spectral densities are maximized for ferromagnetic and weak antiferromagnetic RKKY interactions and they decrease sharply as $I_0/k_B T_K$ grows past the critical ratio. Unfortunately, due to practical limitations,¹³ the number of states kept in those exploratory calculations was insufficient to guarantee good accuracy. In particular, for infinitely separated impurities, the problem becoming equivalent to that described by the single-impurity Hamiltonian, the authors pointed out that the low-

TABLE II. Phase shifts δ and static spectral densities ρ for the indicated ratios of the antiferromagnetic RKKY interaction I_0 , defined in Eq. (21), and the Kondo energy $k_B T_K$. The data were computed for impurity separation $R = \pi/k_F$ and Kondo coupling constant $J = 0.1D$.

$I_0/k_B T_K$	δ_e/π	$(\pi\Gamma_e/2)\rho_e$	δ_o/π	$(\pi\Gamma_o/2)\rho_o$
1.80	-0.500	1.006	0.500	0.999
2.00	-0.500	1.005	0.500	1.001
2.10	-0.500	1.005	0.500	1.000
2.20	-0.500	1.005	0.500	1.000
2.27	-0.500	1.010	0.500	1.000
2.30	0.000	0.000	0.000	0.000
2.50	0.000	0.000	0.000	0.000
3.00	0.000	0.000	0.000	0.000

energy spectral density is 14% smaller than the value predicted by Langreth's (single-impurity) expression.¹ When compared with Eq. (23), the values obtained in the ferromagnetic case display similar deviations, which grow as one moves into the weakly antiferromagnetic regime. Finally, in the strongly antiferromagnetic case, the calculated Fermi-level densities, although small, fail to vanish.

In order to show that a more accurate calculation purges the results of such discrepancies, we have carried out a gen-

eralized NRG computation of the spectral densities for the symmetric model. By fixing the impurity separation at $R = \pi/k_F$ [to make the RKKY coupling I in Eq. (21) equal to zero], fixing the Kondo coupling $J = 0.1D$ and varying I_0 , we then swept the ratio between the (artificial) RKKY interaction and the Kondo temperature through the critical value $I_0/k_B T_K \approx 2.3$.

The results in Table II show that, as expected, the absolute value of the phase shifts drops discontinuously from $\pi/2$ to zero at the critical ratio. The inset in Fig. 1 displays the calculated densities (open squares) as a function of the ratio $I_0/k_B T_K$. The agreement with discontinuous solid line representing Eq. (16) is again excellent.

In summary, we have extended Langreth's exact expression for the Fermi-level spectral density of the single-impurity Anderson model to the Alexander-Anderson model. As an illustration, we compared NRG results with the analytical expression and showed that accurate spectral density computations are within the reach of present computational resources. In particular, the generalized NRG procedure in Ref. 8 was shown to yield excellent agreement with analytical expression for both the asymmetric and the symmetric versions of the model. A study of the energy dependence of the spectral densities will be the subject of a forthcoming report.

This work was supported by the Brazilian agencies FAPESP, CNPq, CAPES, and FINEP.

- ¹D. C. Langreth, Phys. Rev. **B150**, 516 (1966). See also A. Yoshimori and A. Zawadowski, J. Phys. C **15**, 5241 (1982); K. Yamada, Prog. Theor. Phys. **53**, 970 (1975).
- ²J. W. Wilkins, in *Proceedings of the International Conference on Valence Fluctuations*, edited by P. Wachter and H. Boppart (North-Holland, Amsterdam, 1982), p. 1; R. M. Martin, Phys. Rev. Lett. **48**, 362 (1982).
- ³O. Gunnarsson and K. Schönhammer, Phys. Rev. Lett. **50**, 604 (1983); Phys. Rev. B **28**, 4315 (1983).
- ⁴H. O. Frota and L. N. Oliveira, Phys. Rev. B **33**, 7871 (1986).
- ⁵S. Alexander and P. W. Anderson, Phys. Rev. **133**, A1595 (1964).
- ⁶O. Sakai, Y. Shimizu, and T. Kasuya, Solid State Commun. **75**, 81 (1990); Prog. Theor. Phys. **108**, 73 (1992). O. Sakai and Y. Shimizu, J. Phys. Soc. Jpn. **61**, 2333 (1992); **61**, 2348 (1992); O. Sakai, Y. Shimizu, and N. Kaneko, Physica B **188**, 323 (1993).
- ⁷B. A. Jones and C. M. Varma, Phys. Rev. B **40**, 324 (1989); I. Affleck, A. W. W. Ludwig, and B. A. Jones, *ibid.* **52**, 9528 (1995).

- ⁸J. B. Silva *et al.*, Phys. Rev. Lett. **76**, 275 (1996).
- ⁹B. A. Jones, C. M. Varma, and J. W. Wilkins, Phys. Rev. Lett. **61**, 125 (1988).
- ¹⁰R. M. Fye, Phys. Rev. Lett. **72**, 916 (1994).
- ¹¹K. Fischer, Phys. Rev. B **57**, R6771 (1998).
- ¹²J. R. Schrieffer and P. A. Wolff, Phys. Rev. **149**, 415 (1966).
- ¹³The cost of an iterative diagonalization grows rapidly with the number N_s of eigenstates kept in each iteration. In a given iteration L , fixing N_s truncates the spectrum of the Hamiltonian at the energy $E_{trunc} \approx D\Lambda^{-L/2 + \ln(N_s)/(g \ln 2)}$, where $g = 8$ is the degeneracy of a conduction level, and D the halfwidth of the structureless, half-filled band. The relative error in the calculated densities $\rho_p(\epsilon)$ (where $\epsilon \approx D\Lambda^{-L/2}$) predicted by perturbation theory is $D\Lambda^{-L/2}/E_{trunc}$. While the earlier calculations, carried out with $\Lambda = 3$ and $N_s \leq 1000$, yielded 10% deviations (Ref. 6), ours, with $\Lambda = 10$ and $N_s \approx 5000$, yielded less than 1%.
- ¹⁴D. L. Cox, H. O. Frota, L. N. Oliveira, and J. W. Wilkins, Phys. Rev. B **32**, 555 (1985).